Chemical Process Design Vol.1 No.2 (2022) 59-73

University of Sistan and Baluchestan

Chemical Process Design

Available online at http://cpd.usb.ac.ir/

CFD Study on Beds of an Adsorption Desalination System in Order to Improve Bed Performance

Mohamad Hossein Bakhshandeh, Taleb Zarei*, Jamshid Khorshidi

Department of Mechanical Engineering, University of Hormozgan, Bandar Abbas, Iran

ARTICLE INFO

Article history:
Received: 2022-11-30
Received in revised form: 2023-02-02
Accepted: 2023-02-06
Published online: 2023-02-10

Keywords:
Adsorption bed; CFD;
Rectangular finned tube;
Fin thickness; Plates type

DOI: *10.22111/CPD.2023.44116.1015*

ABSTRACT

One of the critical elements of an adsorption desalination system is the adsorption bed. The system dynamics of a 2-bed single-stage silica gel plus water-based adsorption desalination system were analyzed. A great pattern was expanded using energy conservation and mass connected with the kinetics of the adsorption/desorption process. Computational fluid dynamics (CFD) modeling was used to simulate the adsorption process for a rectangular finned tube-based adsorption bed featured with silica gel adsorbent substance. The adsorbents in the simulation were considered solid volume with defined porosity based on the Darcy equation. The adsorption and desorption modes of the adsorption bed was simulated. CFD techniques were then applied to study fin thickness and height. The results showed that decreasing the fin thickness increased the water uptake by up to 8% and decreasing the fin height from 30mm to 20mm increased the water uptake by up to 17%. CFD technique was also used to investigate the effects of plate type on the adsorption bed performance. The results showed that the copper plate improved the water uptake up to 9%. The temperature decline of adsorption bed caused by the copper plate was up to 11% more than that of the aluminum plate

1. Introduction

Nearly 97% of surface water on the earth comprises saltwater which is not drinkable and useful for other purposes. 40% of the world's population currently lives in arid areas where fresh water is rare [1] The hybridization of thermal desalination technologies with renewable energy sources is one of the trends in search and development that seeks to modify the sustainability of these processes [2]. It is possible to segregate soluble salts and other minerals from water using water desalination processes. Feed water sources can be seawater, brackish, groundwater, wastewater, and process water. Recently, adsorption technology has been used for the desalination of water using minimal energy consumption [3, 4]. The main supremacy of adsorption technology is the possibility of using low-grade waste heat sources (50-85°C), solar energy, and environment-friendly refrigerants to lower the cost to one-fifth [5]. The

Corresponding author. Tel.: +98 (917) 362 9158.
E-mail address: talebzarei@hormozgan.ac.ir (T. Zarei).

adsorption desalination system includes four consecutive processes: adsorption, desorption, evaporation, and condensation. Seawater is evaporated in the evaporator via adsorption by the dry adsorbent material along with heat extraction from the chilled water which passes through the evaporator coil and cools down the coil [6]. Water vapor is adsorbed in the adsorption process using adsorbent materials and through desorption. The process includes regenerating water vapor using waste heat. Afterward, the desorbed water vapor is condensed using a condenser to obtain fresh water [8, 9]. Researchers have investigated several adsorption pairs. Silica gel- water double provides a few advantages, mostly in terms of thermal efficiency and environmental trace. Water is an ideal refrigerant due to its high heat of evaporation, thermal consistency at high temperature, and compatibility with a wide range of materials. Silica gel as an adsorbent for water vapor has superior thermal properties of low temperature generation and high adsorption kinetics [10].

Research works on applying numerical simulations have found helpful and efficient techniques for designing adsorption systems and adsorption cycles. Remy et al. [11] simulated an adsorption bed of two layers of packaged beads separated by the steam passage. The results indicate that the adsorption process was governed by heat diffusion resistance and the adsorption process was mainly heat diffusion dependent. Sorption materials compatible with water are silica gel, zeolite, activated alumina to name but a few [12]. Among the important characteristics of sorbents are the ability to absorb a maximum amount of adsorbate per unit mass and a low specific heat. Li et al. [13] studied the modified silica and found out that the improvement of water-resistant performance depends on the decrease of micro-porosity and silanol groups on the silica surface. The diffusion behavior of water vapor on modified silica was determined based on the adsorption equilibrium. The effective diffusivity of water vapor in modified silica was almost the same as in bare silica and decreased by increasing water vapor loading.

Tamainot-Telto et al. [14] described a compact sorption generator based on activated carbon-ammonia pair, which was driven by waste heat obtained from the engine coolant water, giving a cooling power of 1.6kW and COP of 0.22. Boer et al. [15] designed an adsorption chiller and conducted on-board testing, with cooling power enough to maintain convenient temperature levels. Freni et al. [16] studied the dynamics of the water adsorption process by loose silica grains utilizing the CFD method.

Thu et al. [17] examined the efficiency of the ADS using diverse heat recovery designs with two or four-bed modes. The ADS performance was also measured using heat recovery from the condenser to the evaporator or integrated evaporator condenser unit. There was an increase in the evaporator temperature and the adsorption bed pressure because of the heat recovery from the condenser, which created an increase in water production. The increase can be three times higher than the standard ADS.

Researchers have tried to use adsorption technology for water desalination and cooling based on silica gel and several cycle configurations. The performance of a four-bed silica gel adsorption desalination system was examined in an empirical study by Wang et al. [18]. They studied the effects of hot, cold, and chilled water temperatures and cycle duration on the production rate of water cycle and coefficient of performance. The adsorption bed is one of the most significant parts of desalination and the most effective element in the performance of the system. An important part that has not received adequate attention in other research works is the effects of the type of absorbent plates on the adsorption process. Choosing the best material plays an important role in improving the system performance.

Materials with better conductivity improve of the heat transfer process and increase the adsorption coefficient. Absorption process simulation is a very efficient way to obtain the best answer. The effect of different operation

variables (e.g. cooling water flow rate, dry adsorbent desorption time, desorption time, adsorption time, temperatures of evaporation, and condensation) on the performance is an important part of designing a desalination system. However, studies have not paid enough attention to this issue. The adsorption system performance was examined with different cycle times, heat fluid temperatures, and flow rates. In addition, the effect of different adsorber bed fin numbers and fin height were examined using the model.

Simulation techniques are efficient tools in investigating the adsorption process and modifying the designs of adsorption beds. CFD technique was used to examine the effects of plate types on the performance of the adsorption bed. Here, a finite element model was introduced to simulate the adsorption process of various adsorption beds. Other studies have failed to examine adsorption bed configurations with different plate types. In the present study, a CFD model was designed considering the inter/intra grain mass transfer resistances and time-depended evaporation pressure. A rectangular finned tube heat exchanger filled with adsorbent particles was investigated. The effects of spatial porosity on the performances of the adsorption cycle and the water production were also studied. Moreover, both of the adsorption and the desorption modes of the system were simulated.

A numerical investigation was conducted on the performance of a prototype adsorption desalination (AD) plant. The key objective was to propose a design and CFD simulation of a novel compacted copper fin heat exchanger with a silica gel adsorbent bed that constitutes a part of the adsorption system. The proposed heat exchanger design is featured with a wide surface area. By estimate, this surface helps to improve the coefficient of performance (COP) of the adsorption phase. It also improves heat transfer in this system arrangement [19].

1.1. Mechanism of the present bed adsorption system

Almost every adsorption system relies on a two-bed cycle (Fig. 1). The thermodynamic cycle is demonstrated in Fig.1. There are two adsorber beds in a two-bed cycle system and these beds function in opposite modes. Mainly, during the switching, while an adsorber is in a preheating process, the other one is in a precooling process.

The system includes an evaporator, two adsorption beds, and one condenser. Its function features two processes: adsorption and desorption. When repeated one after another, the system produces desalinated water. Based on this design, the condenser and evaporator are connected to the adsorption beds. During desorption, the control valve connects the beds to the condenser. In addition, desalinated water is collected in a tank. The process cycle is completed by connecting the evaporator to the absorption bed. Following adsorption bed saturation, the control valves connecting the adsorption bed and the evaporator are closed. Then, the adsorption bed is heated by the heat exchangers. The temperature and pressure of the adsorption bed increase in the heating process. There is a connection between the adsorption bed and the condenser so that the vapor is condensed by its heat exchangers.

2. Adsorption isotherm models

The adsorption isotherm clarifies the amount of adsorbate adsorbed using the adsorbent at a given temperature. The adsorbate mass normalization with the absorbent mass for different materials allows the collation of absorption capability. In this way, we make sure that by implementing the saturation pressure the adsorption stops because of the limited capacity of the empty holes on the surface of the adsorbent. The linear driving force equation (LDF) is the first choice to describe the adsorption kinetics of adsorption working couples. However, there are different adsorption isotherm equations available [20].

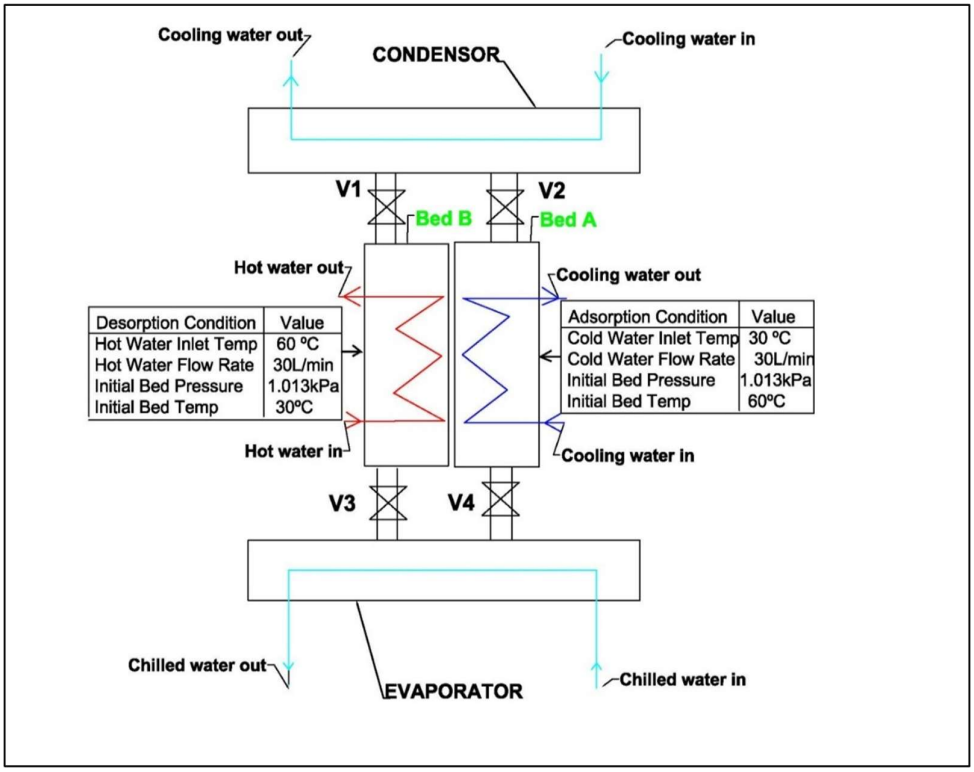

Fig. 1. Two-bed adsorption desalination cycle system

Adsorption processes can be applied in applications like separation and air-conditioning. It relies on water vapor physical uptake on the surface of the adsorbent based on Van der Waal's or polar bonding forces (e.g., silica gel, and zeolite). Evaporation of pre-treated seawater happens via the suction from the adsorbent which does not need high pressure or temperature. After the adsorption of the vapors by the adsorbent, the adsorption heat is returned to the cooling water circuit and the adsorber bed. This adsorption process goes on while the cycle time is not over. For adsorbent regeneration, the bed is supplied with low-temperature waste at the onset of the desorption mode. Then the bed is connected to the condenser where the water vapor condensation on the cooler tube surfaces happens and water is collected on the reservoir.

2.1. Computational domain of the simulated adsorption bed

Rectangular finned tube adsorption beds are available in the market with tubes and rectangular fins (Fig. 2). The bed design utilized in silica gel/water adsorption system was manufactured by Weatherite [20]. Distribution of the fins is uniform over the length of the tubes. To lower the adsorption bed mass, the fins are made of aluminum. The fins dimensions are 75×30×0.105mm and an extra four tubes were uniformly distributed over the width of the adsorption bed. The external diameter of the bed is 15.8mm and thickness of wall is 0.8mm. To have a higher thermal conductivity, copper tubes are used. In addition, adsorbent granules were packed between the fins. The cooling water in the adsorption process grows through tubes and decreases the temperature of the adsorption bed and compensates the heat of the desorption process (Table 1) The cooling water in the adsorption process goes through the tubes to decrease the temperature of the adsorption after the desorption process. In addition, silica gel granules are added between fins. The boundary conditions require a fixed evaporation pressure on the interface of adsorbent material and the sides and the underside surfaces.

Table 1. Bed design parameters

Symbol	Value	Description
L_f	100mm	Bed length
W_f	75mm	Fin width
H_f	30mm	Fin height
P_f	1.5mm	Fin pitch
t_f	0.105mm	Fin thickness
D_o	15.8mm	Tube outer diameter
t_t	0.8mm	Tube thickness

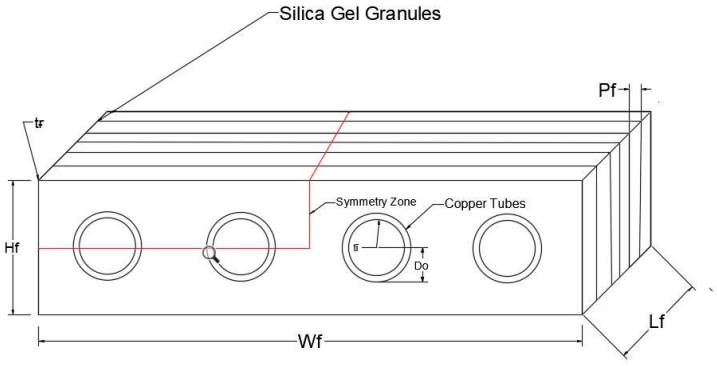

Fig. 2. Rectangular finned tube adsorption bed

3. CFD model

Eq. (1) presents the Darcy equation that justifies the continuity of the adsorption process and Eq. (2) represents the energy equation.

$$\frac{\partial(\varepsilon_s \rho_w)}{\partial t} + \nabla.(\rho_w u_w) = -\frac{\partial(\rho_s w)}{\partial t} \tag{1}$$

$$\rho C_P \frac{\partial T_{bed}}{\partial t} + C_{P_w} \nabla.(T_{bed} \rho_w u_w) = \nabla.(k_s \nabla T_{bed}) + \rho_s \Delta H_s \frac{\partial w}{\partial t} \tag{2}$$

$$u_w = -\frac{\kappa}{\mu} \nabla P_w \tag{3}$$

$$\rho C_p = (\varepsilon_s \rho_w + \rho_s w) C_{P_w} + \rho_s C_{P_s} \tag{4}$$

where ε_s is porosity of adsorbent bed packed with silica gel granules equal to 0.5 [22], u_w represents water vapor velocity (Eq. (3)), ∇P_w represents water vapor pressure gradient, ρC_P is obtained by Eq. (4), and k_s is the thermal conductivity of the bed equal to 0.198W/(m.K), and κ is the permeability of silica gel determined by Eq. (5).

$$k = -\frac{4\varepsilon_s^3 R_P^2}{150(1-\varepsilon_s)^2} \tag{5}$$

where w is the uptake value of the water vapor by silica gel, which is obtained by the linear driving force (LDF) of the kinetic model (Eqs. (6-7)).

$$\frac{dw}{dt} = K\left(w_{\max} - w\right) \tag{6}$$

$$K = 15 D_{SO} \exp(\frac{-E_a}{RT_{bed}}) / R_P^2 \quad (7)$$

where $w_{\max}$ is the maximum water vapor uptake of silica gel granules at the equilibrium condition. For Eq. (6), K is the overall mass transfer rate of the silica gel-water pair which can be calculated using Eq. (7), where D_{SO} represents the pre-exponential constant, E_a stands for the activation energy, R_P stands for the silica gel granule radius, and R is the ideal gas constant (Table 2).

Table 2. Parameters for mass transfer rate equation

Parameter	value	Unit
D_{SO}	2.54×10^{-4}	m^2/s
E_a	4.2×10^{-4}	J/mol
R_P	0.15×10^{-3}	m
R	8.314	J/(mol.K)

The modified Freundilich model (Eqs. (8-10)) and Table 3 lists the values of constants [21].

$$w_{\max} = A\left[\frac{PT_e}{PT_{bed}}\right]^B \quad (8)$$

$$A = A_0 T_{bed} + A_1 T_{bed} + A_2 T_{bed}^2 + A_3 T_{bed}^3 \quad (9)$$

$$B = B_0 T_{bed} + B_1 T_{bed} + B_2 T_{bed}^2 + B_3 T_{bed}^3 \quad (10)$$

Table 3. Constants for equilibrium uptake equation [23]

Parameters	Value	Unit
A_0	-6.531	$kg_{water}/kg_{silicagel}$
A_1	7.24×10^{-2}	$kg_{water}/(kg_{silicagel}.K)$
A_2	-2.39×10^{-4}	$kg_{water}/(kg_{silicagel}.K^2)$
A_3	-2.54×10^{-7}	$kg_{water}/(kg_{silicagel}.K^3)$
B_0	−15.58	1
B_1	0.159	K^{-1}
B_2	-5.06×10^{-4}	K^{-2}
B_3	-5.3×10^{-7}	K^{-3}

3.1. Boundary conditions and grid study

The thermal and flow variables on the boundaries of the physical model were determined by the boundary conditions. The boundary conditions are:

- Flow outlet and inlet to boundaries: velocity inlet, pressure inlet, and pressure outlet.
- Recurring wall, and limit boundaries: wall, symmetry internal fluid, solid.
- Internal face boundaries: wall, porous
- Internal fluid, solid
- The system operates under isothermal condition.
- Negligible pressure drops through the adsorbent bed.
- Langmuir isotherm is valid for the system.
- Ideal plug flow is assumed; (there is no axial or radial dispersion).
- The mass transfer rate is represented by a linear driving force expression.

Initial and boundary conditions:

$$\varepsilon\frac{\partial C}{\partial t}+u\frac{\partial C}{\partial z}+(1-\varepsilon)\rho_a\frac{\partial w}{\partial t}=D_z\frac{\partial^2 C}{\partial z^2} \tag{11}$$

$$t=0\rightarrow C(z,t)=0 \tag{12}$$

$$t=0\rightarrow w(z,t)=0 \tag{13}$$

$$z=0\rightarrow C(0,t=0)=0\ ,\ C(0,t>0)=C_F \tag{14}$$

$$z=H\rightarrow\frac{\partial C}{\partial z}=0 \tag{15}$$

when the axial dispersion is ignored,

$$\varepsilon\frac{\partial C}{\partial t}+u\frac{\partial C}{\partial z}+(1-\varepsilon)\rho_a\frac{\partial w}{\partial t}=0 \tag{16}$$

whereas C is the concentration in fluid phase (kg/m^3), ε is the bed porosity, ρ_a is adsorbent density (kg/m^3), w is adsorbed phase concentration (kg adsorbed/kg of adsorbent). The mass transfer kinetics is modeled using the LDF, Linear driving force approximations:

$$\frac{\partial w}{\partial t}=\frac{15D_S}{R_P^2}(w_{\max}-w) \tag{17}$$

$$D_S=D_{S0}\exp(\frac{-E_a}{RT_{bed}}) \tag{18}$$

The initial and boundary conditions turn to:

$$t=0\rightarrow C(z,t)=0 \tag{19}$$

$$z=0\rightarrow C=C_F+\frac{D_z\varepsilon}{u}\frac{\partial C}{\partial z} \tag{20}$$

$$z=H\rightarrow\frac{\partial C}{\partial z}=0 \tag{21}$$

where ε is the bed porosity, t is time, ρ_a is the adsorbent density, C_F is the initial concentration of the inlet, and H is the bed height. In the case of the geometry under study, a set of grids was used with CFD computations and the effects of each grid level was analyzed afterwards. To solve the problem, we need a systematic gridding known as the grid convergence or mesh refinement. Fig. 3 illustrates mesh grid size with three mesh types (large-medium-fine) including coarse to dense meshes generated to make sure that the simulation results were adequately grid-independent.

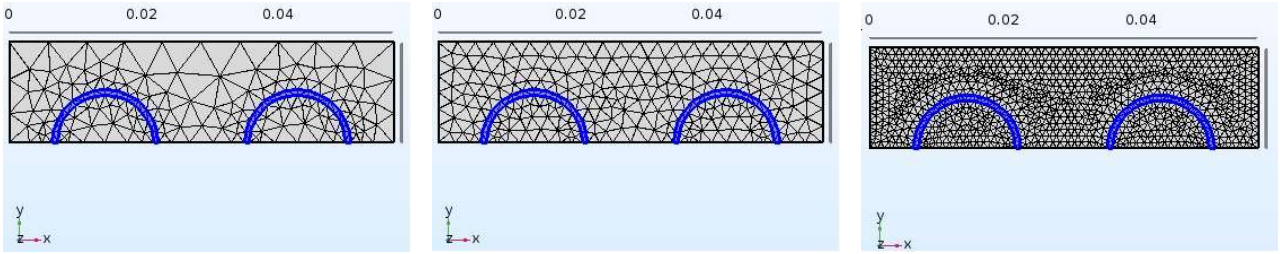

(a) Number of mesh size: 232,000 (b) Number of mesh size: 514,000 (c) Number of mesh size: 951,000

Fig. 3. Mesh grid size (a) large grid, (b) medium grid, (c) fine grid

The bed temperature results are shown in Fig. 4. The results show that the two types of mesh grid (medium and fine grid) were very similar and the error level was less than 3%. Medium mesh is used for simulation and save time and energy.

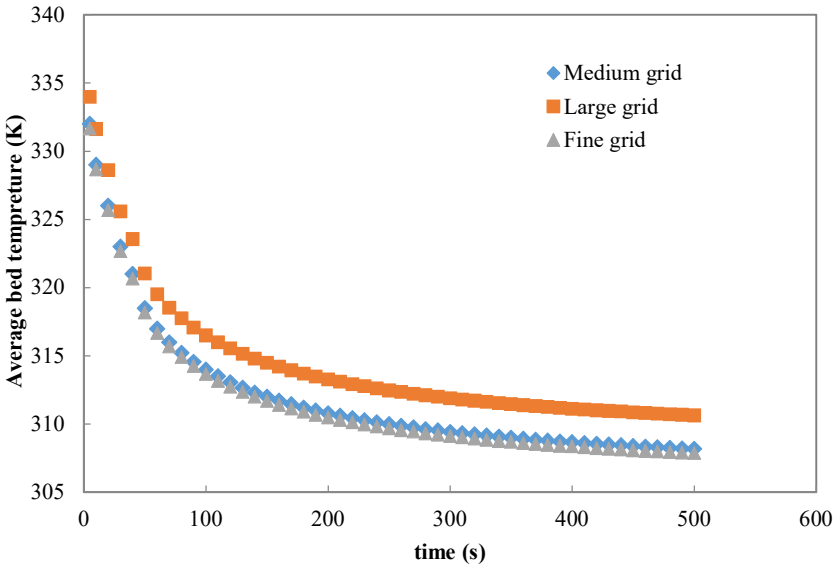

Fig. 4. Three mesh types analysis with different sizes (large- medium-fine)

4. Results and discussion

4.1. Model validation

The simulation model was validated by applying the experimental results [21]. The difference between the experimental data and simulation result is shown in Fig. 5 and clearly the difference is less than 5%. Fig. 5 illustrates the simulated and experimental results, including average bed temperature, water uptake, and cooling water outlet temperature in an adsorption cooling system based on a SAPO-34/water working pair. The results indicate a good consistency between the finite element model and the experiments.

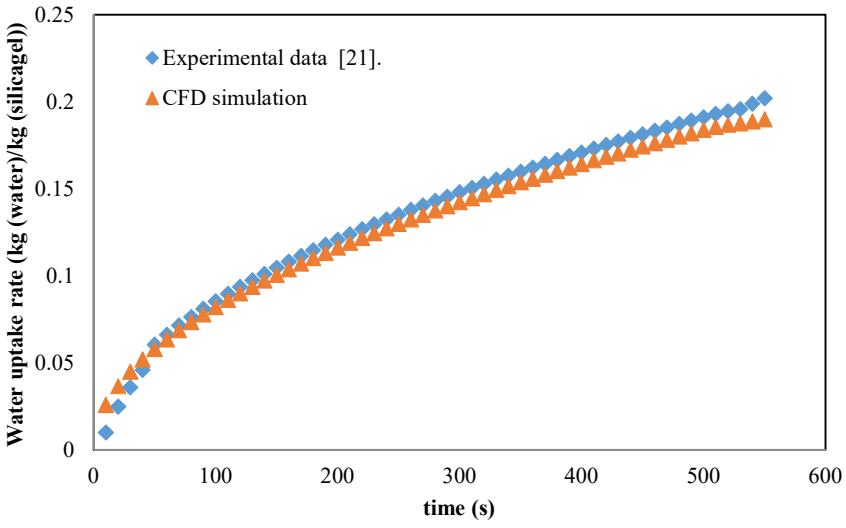

Fig. 5. Comparison of water vapor uptake between CFD predicted data and experimental data (volume flow rate of 5L/min)

4.2. Adsorption mode

To examine the adsorption process of adsorption bed featured with rectangular finned tube based on CFD modeling technique, a simulation was performed (inlet water temperature of 30˚C, evaporator temperature of 15˚C, and initial bed temperature of 60˚C). The complete adsorption process took 500s, which allowed us to predict the adsorption performance of adsorption bed of silica gel-water working pair.

Fig. 6(a) shows the predicted temperature distribution on the fins of the rectangular finned tube adsorption bed versus time. The bed temperature is the adsorption bed's average temperature, which includes the metal and silica gel granules. As the simulation time passes, the bed temperature converges to the coolant temperature. The temperature difference between the cooling water which cools the bed in adsorption mode is higher at the beginning of the process.

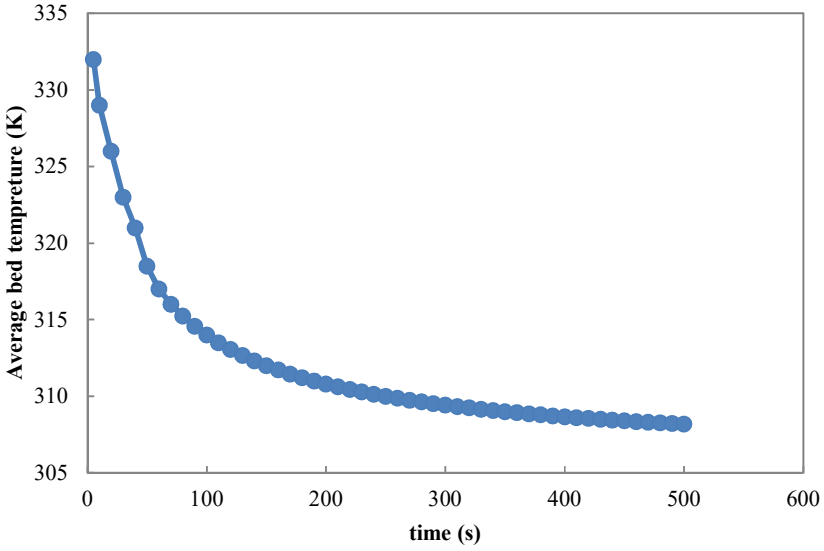

(a)

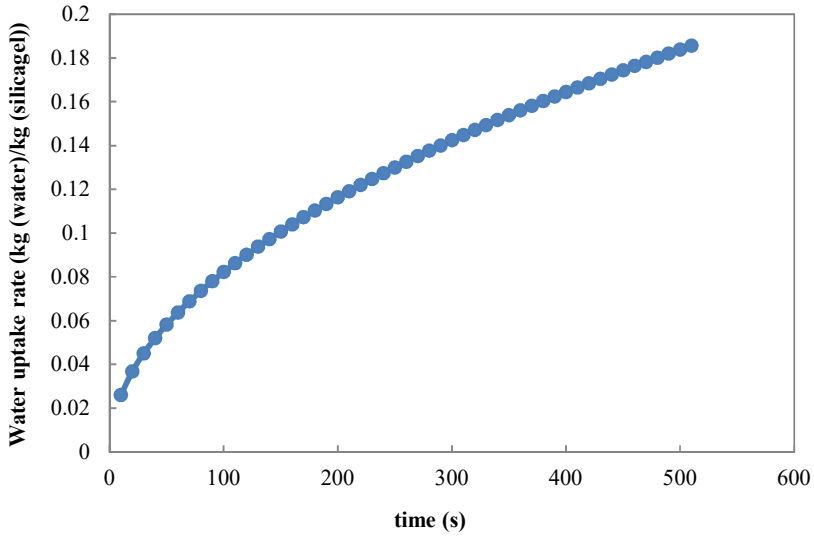

(b)

Fig. 6. Simulation results for adsorption process versus time (a) average bed temperature, (b) water uptake rate

Specifically, in the adsorption process, the average bed temperature decreases with the increase of time. This increase is with a sharp slope between the times from 0 to 200 seconds. This could be because the adsorbents have a high adsorption capacity at the beginning of the process, which accelerates the process. The driving force is more active at the beginning of the process, which accelerates the process. As time passes, the adsorption capacity of the adsorbents decreases and the process becomes slower.

The predicted water uptake rate of plane was investigated at the time interval 0 to 500s. Obviously, when the desorption process occurs, the water uptake rate increases with longer simulation time. This is because that desorption process is fast between 50^{th}s and 300^{th}s at the beginning and deaccelerates from 200^{th}s to 500^{th}s. Another reason is that the system reaches saturation and loses its absorption capacity over time. The water outlet temperature is the cooling water temperature at the outlet of tubes which is heated by the initial hotbed and the adsorption heat. The temperature of the bed decreases when the bed loses energy in the adsorption process.

4.3. Desorption mode

Fig. 7(a) shows the predicted average bed temperature of the adsorption bed at time intervals of 0 to 500 seconds. Clearly, during the desorption process, the average bed temperature increases with time. During the heating phase, the rate of heat increase is high and the temperature of the bed increases at a faster rate. However, as the bed temperature rises, the temperature difference between circulating hot water and the adsorber bed decreases and as a result, the rate of heat transfer and the rate of temperature rise both decrease. The slope of the curve becomes almost zero after 400 seconds. The reason for this is that after 400 seconds, the system reaches the temperature equilibrium and the adsorption bed temperature remains almost constant.

In the desorption process, the average temperature of silica gel increases with an increase in the temperature of copper pipes. The absorbed water is released by heating and the water uptake rate of the plane increases. In addition, this process occurs in the adsorption phase; however, when the bed temperature decreases the vapor of the bed adsorption by silica gel increases.

Fig. 7(b) illustrates the predicted water uptake rate of the plane at time intervals of 0 to 500 seconds. At the start of the desorption process, the adsorbents store a high capacity of water, which desorb this amount of water by receiving heat from the system. The rate of desorption tends to increase due to an increase in bed temperature; however, it tends to decrease due to progressively lower value of adsorbed mass and also due to lower rate of heat transfer. The net result of these effects decreases the rate of desorption very slowly. Clearly, when the desorption process occurs, water uptake rate decreases with time. This is because that the desorption process is fast at the beginning (from 50^{th}s to 300^{th}s) and deaccelerates between 400^{th}s to 500^{th}s. After 400s the system reaches an equilibrium and the changes in water uptake rate becomes insignificant. The mass transfer, which is a function of time, either inside or outside of the porous adsorbent is triggered by its adsorption and desorption rate adjusted by the user. The function is used to solve the Eq. (1) for desorption and adsorption of water vapor [24].

The horizontal cut plane of temperature distribution of the last fin in desorption phase is shown in Fig. 8(A). The predicted temperature distribution of the plane was investigated at time intervals of 1, 50, 100, 200 seconds. Clearly, the temperature becomes larger with the increase of time. Fig. 8(B) shows the horizontal cut plane of temperature distribution of the last fin in adsorption. The predicted temperature distribution of the plane was examined at time intervals of 1, 50, 100, 200 seconds. Clearly, the temperature decreases in time. The water outlet temperature is the

heating water temperature at the outlet of tubes which is cooled by the initial cold bed and the heat loss of desorption. The desorption process occurs when the bed gains energy and the temperature of the bed increases.

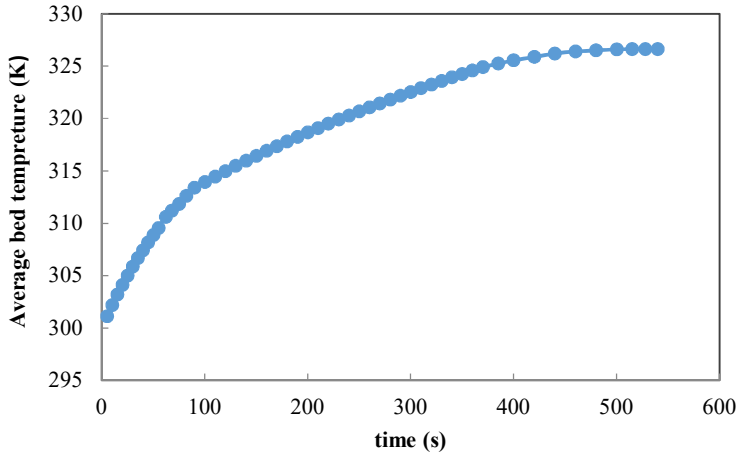

(a)

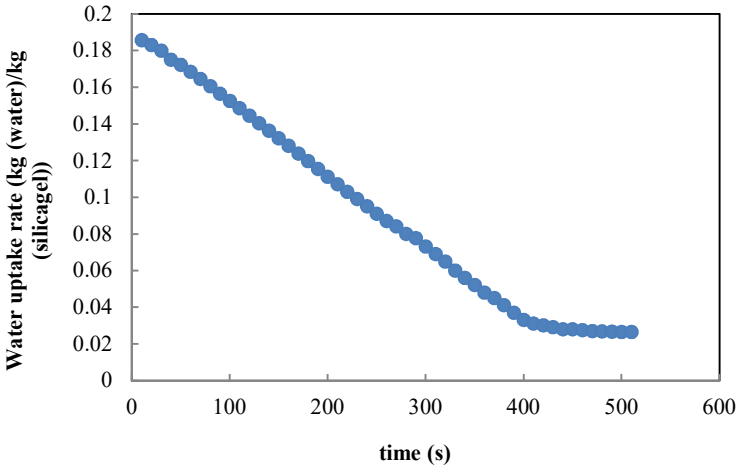

(b)

Fig. 7. Simulation results for desorption process: (a) average bed temperature, (b) water uptake rate

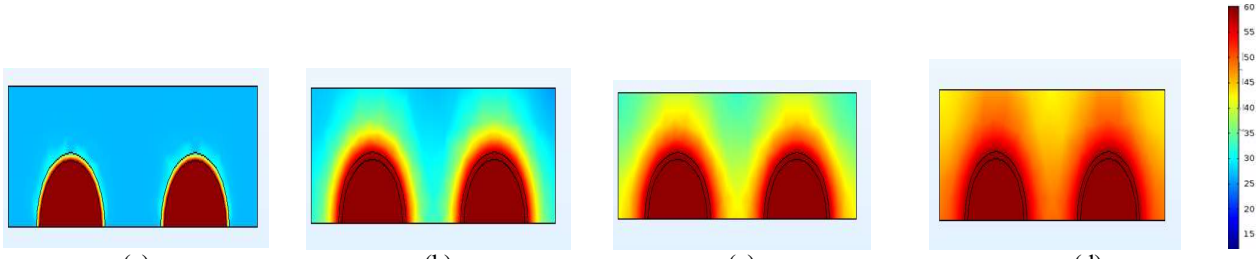

(a) (b) (c) (d)

(A)

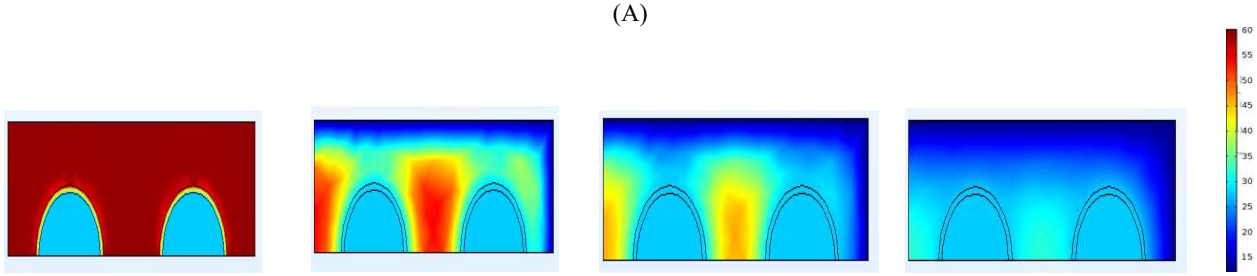

(a) (b) (c) (d)

(B)

Fig. 8. Temperature distribution of the last fin at (a) 1s; (b) 50s; (c) 100s; (d) 200s for desorption (A) and for adsorption (B)

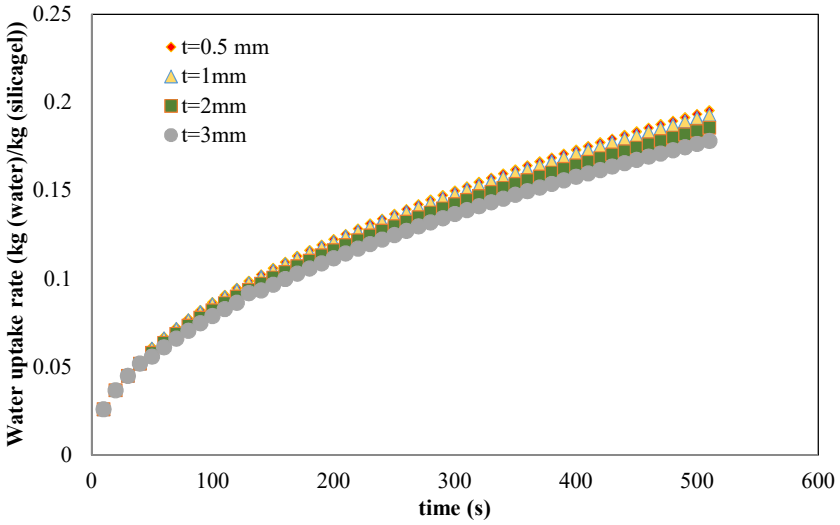

Fig. 9. Simulation results for water uptake rate with different fin thickness

The water uptake rate increases by decreasing the fin thickness. Clearly, water uptake rate for fin thickness of 1mm and 0.5mm is higher than the others. Since the output data from a thickness of less than 1mm is almost the same, the same thickness is selected for the simulation. This can be attributed to the fact that with decreasing the fin thickness, the amount of the adsorbent increases; hence, the ratio between the adsorbent and the metal mass also increases causing a poorer heat transfer rate. The results showed that decreasing the fin thickness increases the water uptake by up to 8%. This can improve system performance as reducing the thickness of plates increases the heat transfer rate.

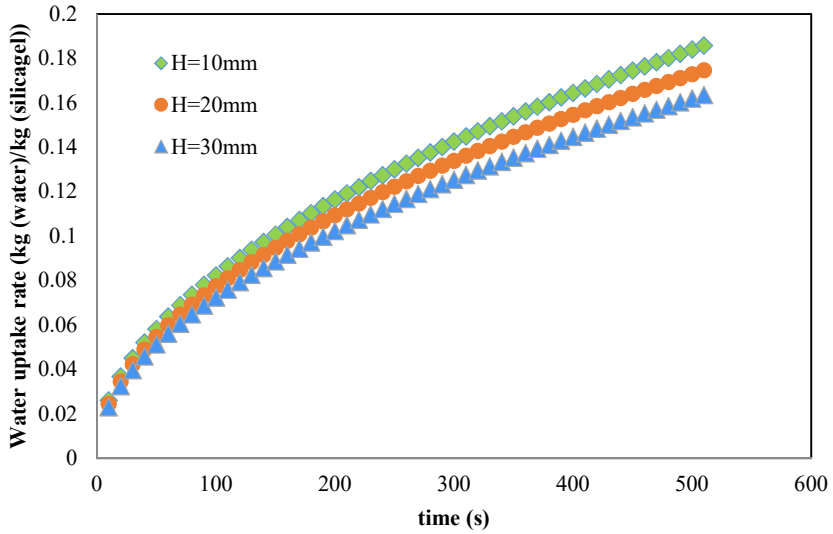

Fig. 10. Simulation results for water uptake rate with different fin heights

Fig. 10 shows that the water uptake rate increases with decreasing the fin heights. It is clear that water uptake rate for fin heights of 10mm is higher than the others. Decreasing the fin height from 30mm to 10mm results in increasing

the water uptake by up to 17%. This can be due to the increase in the number of fins and the heat transfer area thus cooling the bed more effectively and increasing the water adsorption by the silica gel.

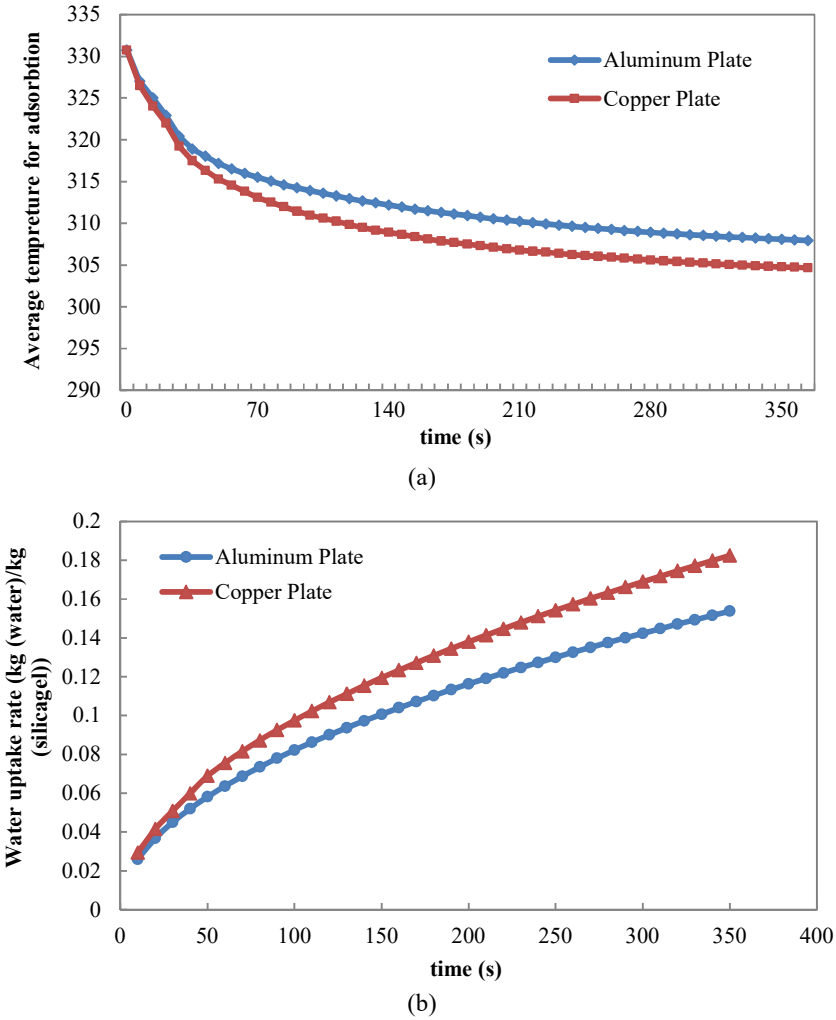

Fig. 11. Simulation results for adsorption process with different plates types (a) average bed temperature, (b) water uptake rate

One of the new features of the present study is to compare the result of simulation with different plate types (aluminum plate and copper plate). Because of the difference in the heat transfer coefficient of copper and aluminum, the effect of material change on the performance of plates in the adsorption process was investigated for the first time. Fig.11(a) shows the adsorption process with an initial bed temperature of 303K and a hot water temperature of 331.4K. Time duration of the process was about 350s. During the adsorption process, the bed temperature decreases, and hence the temperature difference between the bed and the cooling water also decreases. Therefore, heat transfer rate and hence the rate of temperature drops decrease during this process. The results showed that copper plates had a better adsorption. It is clear that copper plate decreased the temperature of the bed by about 11%. The CFD technique was used to examine the effects of plate types on the performance of adsorption bed. The results showed that copper plate increased the water uptake up to 9%. Fig. 11(b) shows that the copper plate has a better performance in increasing water uptake rate.

The CFD simulation demonstrated that the heat transfer proficiency of the silica gel adsorption bed was a significant factor in the adsorption output of the bed. To have a clear picture of heat transfer performance of the silica gel, the

surface temperature of the silica gel was determined in the simulation. The water temperature (50°C and 70°C) was used to adjust the silica gel surface temperatures and have a better picture of the transfer performance of adsorbent bed with silica gel.

5. Conclusion

The CFD simulations technique proved to be a powerful tool to examine the adsorption process and improve the designs of adsorption beds. An adsorption process for a silica gel-water pair in a rectangular finned tube bed structure that can be used for the adsorption desalination system was investigated. The bed geometry and the adsorption process of working pair were modeled using CFD techniques in COMSOL Multiphysics. The simulations were used to investigate the bed performance of the adsorption process. CFD technique was used to examine the effects of fin thickness and fin height on the performance of adsorption bed. The results showed that decreasing the fin thickness increased the water uptake up to 8%. In addition, decreasing the fin height from 30mm to 20mm increased the water uptake up to 17%. The effects of plate types on the performance of the adsorption bed were examined using CFD technique. The results showed that copper plate improved the water uptake up to 9%. Moreover, the copper plate decreased the temperature of adsorption bed up to 11% more than the aluminum plate. In conclusion, CFD is a valuable tool to examine the heat transfer behavior of an adsorption bed. Future studies on CFD can use bigger silica gel and porous media.

Nomenclature

Symbols	
A_0-A_3	Constant coefficients for equation 9
B_0-B_3	Constant coefficient for equation 10
C	Concentration in fluid phase, kg/m^3
C_F	Initial concentration, kg/m^3
C_p	Specific heat, J/(kg.K)
C_{so}	Pre-exponential constant
d	Diameter, m
E_a	Activation energy, kJ/mol
D_{SO}	Pre-exponential factor of the effective water diffusivity, m^2/s
D_S	Surface diffusivity, m^2/s
D_o	Tube outer diameter, mm
H_f	Fin height, mm
ΔH	Heat of adsorption, kJ/mol
k	Thermal conductivity, W/(m.K)
K	Overall mass transfer rate, kg/s
M	Mass, kg
N	Number
P	Pressure, kPa
P_f	Fin pitch, mm
R	Ideal gas constant, J/(mol.K)
R_P	Silica gel granule radius, m
t_f	Fin thickness, mm
t_t	Tube thickness, mm
T	Temperature, °C
u	Velocity (m/s)
w	Water uptake rate, g_{ref}/g_{ads}
w_f	Fin width, mm
Abbreviation	
ADS	Adsorption desalination system
CFD	Computational fluid dynamics
COP	Coefficient of performance
LDF	Linear driving force
Greek symbols	
ρ	Density, kg/m^3
κ	Permeability of silica gel
ε	Bed porosity
μ	Gas dynamic viscosity (Pa.s)
Subscript	
bed	Adsorption bed
i	Inside of tubes
max	Maximum value
o	Outside of tubes
out	Water outlet
s	Packed silica gel granules
t	Tube
w	Water vapor

References

[1] Harby, K., Ali, E.S., Almohammadi, K.M., 2021. A novel combined reverse osmosis and hybrid absorption desalination-cooling system to increase overall water recovery and energy efficiency, Journal of Cleaner Production, 287, 125014-125024. https://doi.org/10.1016/j.jclepro.2020.125014
[2] Feria-Díaz, J.J., López-Méndez, M.C., Rodríguez-Miranda, J.P., Sandoval-Herazo, L.C., Correa-Mahecha, F., 2021. Commercial thermal technologies for desalination of water from renewable energies: A state of the art review, Processes, 9(2), 262-273. https://doi.org/10.3390/pr9020262
[3] Amirfakhraei, A., Zarei, T., Khorshidi, J.J.T.S., 2020. Performance improvement of adsorption desalination system by applying mass and heat recovery processes, Thermal Science and Engineering Progress, 18, 100516-100527. https://doi.org/10.1016/j.tsep.2020.100516
[4] Majdi, M.S., Al-Dadah, R., Mahmoud, S., Elsayed, E., El-Samni, O., 2020. Wire fin heat exchanger using aluminium fumarate for adsorption heat pumps, Applied Thermal Engineering, 164, 114426-114437. https://doi.org/10.1016/j.applthermaleng.2019.114426
[5] Shakib, S., Amidpour, M., Ghafoorian, M.M., 2019. Optimization of a Hybrid Multi-effect Desalination with Thermal Vapor Compression and Reverse Osmosis Desalination System Integrated to A Gas Turbine Cycle, Amirkabir Journal of Mechanixal Engineering, 50(6), 1333-1350. https://doi.org/10.22060/MEJ.2017.12982.5491
[6] Verde, M., Cortés, L., Corberán, J., Sapienza, A., Vasta, S., Restuccia, G.J.A.T.E., 2010. Modelling of an adsorption system driven by engine waste heat for truck cabin A/C. Performance estimation for a standard driving cycle, 30(13), 1511-1522. https://doi.org/10.1016/j.applthermaleng.2010.04.005
[7] Srivastava, N., Eames, I.J.A.t.e., 1998. A review of adsorbents and adsorbates in solid–vapour adsorption heat pump systems, Applied Thermal Engineering, 18(9-10), 707-714. https://doi.org/10.1016/S1359-4311(97)00106-3
[8] Youssef, P.G., Mahmoud, S., Al-Dadah, R.K., 2015. Effect of evaporator temperature on the performance of water desalination/refrigeration adsorption system using AQSOA-ZO2, World Academy of Science, Engineering and Technology, International Journal of Environmental, Chemical, Ecological, Geological and Geophysical Engineering, 9(6), 701-705. https://www.scinapse.io/papers/2621193895
[9] Saha, B., Koyama, S., Kashiwagi, T., Akisawa, A., Ng, K.C., Chua, H.J.I.J.o.R., 2003. Waste heat driven dual-mode, multi-stage, multi-bed regenerative adsorption system, International Journal of Refrigeration, 26(7), 749-757. https://doi.org/10.1016/S0140-7007(03)00074-4
[10] Chua, H.T., Ng, K.C., Malek, A., Kashiwagi, T., Akisawa, A., Saha, B.J.I.j.o.R., 1999. Modeling the performance of two-bed, sillica gel-water adsorption chillers, International Journal of Refrigeration, 22(3), 194-204. https://doi.org/10.1016/S0140-7007(98)00063-2
[11] Mohammed, R.H., Mesalhy, O., Elsayed, M.L., Chow, L.C., 2017. Novel compact bed design for adsorption cooling systems: parametric numerical study, International Journal of Refrigeration, 80, 238-251. https://doi.org/10.1016/j.ijrefrig.2017.04.028
[12] Saliba, S., Ruch, P., Volksen, W., Magbitang, T.P., Dubois, G., Michel, B., 2016, Combined influence of pore size distribution and surface hydrophilicity on the water adsorption characteristics of micro-and mesoporous silica, Microporous and Mesoporous Materials, 226, 221–228. https://doi.org/10.1016/j.micromeso.2015.12.029
[13] Stefanski, S., Nowak, W., Sztekler, K., Kalawa, W., Siwek, T., 2019. Applicability of adsorption cooling/desalination systems driven by low- temperature waste heat, IOP Conference Series: Earth and Environmental Science, 214, 121-126. https://doi.org/10.1088/1755-1315/214/1/012126
[14] Tamainot-Telto, Z., Metcalf, S.J., Critoph, R.E.J.I.J.o.R., 2009. Novel compact sorption generators for car air conditioning, International Journal of Refrigeration, 32(4), 727-733. https://doi.org/10.1016/j.ijrefrig.2008.11.010
[15] Vasta, S., Freni, A., Sapienza, A., Costa, F., Restuccia, G.J.I.J.o.R., 2012. Development and lab-test of a mobile adsorption air-conditioner, International Journal of Refrigeration, 35(3), 701-708. https://doi.org/10.1016/j.ijrefrig.2011.03.013
[16] Freni, A., Maggio, G., Cipitì, F., Aristov, Y.I.J.A.T.E., 2012. Simulation of water sorption dynamics in adsorption chillers: One, two and four layers of loose silica grains, Applied Thermal Engineering, 44, 69-77. https://doi.org/10.1016/j.applthermaleng.2012.03.038
[17] Thu, K., Chakraborty, A., Kim, Y.-D., Myat, A., Saha, B.B., Ng, K.C.J.D., 2013. Numerical simulation and performance investigation of an advanced adsorption desalination cycle, Desalination, 308, 209-218. https://doi.org/10.1016/j.desal.2012.04.021
[18] Wang, D., Zhang, J., Tian, X., Liu, D., Sumathy, K.J.R., Reviews, S.E., 2014. Progress in silica gel–water adsorption refrigeration technology, Renewable and Sustainable Energy Reviews, 30, 85-104. https://doi.org/10.1016/j.rser.2013.09.023
[19] Shi, B., AL-Dadah, R., Mahmoud, S., Elsayed, A., Rezk, A.J.P.o.I., 2013. Mathematical and CFD modelling for a rectangular finned tube adsorption bed for automotive cooling system, International Conference on Applied Energy ICAE 2013, Jul 1-4, 2013, Pretoria, South Africa.
[20] Ali, S.M., Chakraborty, A.J.E.C., 2016. Adsorption assisted double stage cooling and desalination employing silica gel+ water and AQSOA-Z02+ water systems, Energy Conversion and Management, 117, 193-205. https://doi.org/10.1016/j.enconman.2016.03.007
[21] Alsaman, A.S., Askalany, A.A., Harby, K., Ahmed, M.S.J.E., 2017. Performance evaluation of a solar-driven adsorption desalination-cooling system, Energy, 128, 196-207. https://doi.org/10.1016/j.energy.2017.04.010
[22] Lu, T.J., 1999. Heat transfer efficiency of metal honeycombs, International Journal of Heat and Mass Transfer, 42(11), 2031-2040. https://doi.org/10.1016/S0017-9310(98)00306-8
[23] Sharafian, A., Bahrami M.J.R., 2014. Assessment of adsorber bed designs in waste-heat driven adsorption cooling systems for vehicle air conditioning and refrigeration, Renewable and Sustainable Energy Reviews, 30, 440-451. https://doi.org/10.1016/j.rser.2013.10.031